XLVI CILAMCE
VITÓRIA - ES - BRAZIL - 2025
XLVI IBERO-LATIN AMERICAN CONGRESS ON COMPUTATIONAL METHODS IN ENGINEERING

Fiber orientation optimization for mitigating stress concentration factors in perforated composite leaf-springs

G. Binkowski Perroni[1,2], D. Milbrath De Leon[1]

[1]*Mechanical Engineering Department*, *Universidade Federal do Rio Grande do Sul*
90035- 190- Centro Histórico, Porto Alegre – RS
[2]*Hercílio Randon Institute, Francisco Getúlio Vargas Street, 95070-560 -Caxias do Sul - RS*
guilherme.perroni@ufrgs.br, daniel.leon@*ufrgs.br*

Abstract. Advances in composite materials are enabling the replacement of traditional steel leaves in heavy duty vehicle suspension springs with composite ones. By means of analytical simulations written in Python and grounded in classical lamination theory, this study evaluates spring leaves at three fiber volume fractions (V_f = 50 %, 60 %, 70 %) composed of epoxy resin and basalt fiber, showing how systematic variation of fiber orientation and V_f governs axial stiffness, in plane and out of plane moduli, anisotropy ratios, transverse Poisson's ratio, and stress concentration factors around the central circular discontinuity. Results indicate that optimizing V_f from 70 % down to 60% does not significantly alter stiffness while preserving reduced stress amplification within specific orientation windows, thereby providing practical guidelines for designing lighter high performance suspension components, highlighting the Topology optimization role in such designs.

Keywords: Composite Material; Fiber Orientation; Stress Concentration Factor, Topology Optimization.

1 Introduction

Composite materials unite two or more distinct phases to achieve mechanical capabilities that exceed those of the individual constituents. Their overall response is interpreted through macromechanics, while micromechanics clarifies local constituent interactions (Chawla [1]). Structural features such as openings act as stress concentrators: the longitudinal spring analyzed here includes a centrally drilled hole that permits attachment to the vehicle's chassis assembly but also concentrates stresses.

Growing interest in composite suspensions reflects the drive for efficiency and sustainability. The Society of Automotive Engineers Spring Design from SAE [2] still underpins calculations of load, deflection and fatigue, even when steel is supplanted by lighter composites. Building on these fundamentals, Ke [3] surveyed material choices, design strategies and performance metrics for composite leaf springs; Tadesse and Fatoba [4] showed that composite springs in heavy-duty trucks cut weight and boost fuel economy; and Telli [5] assessed composite beams under combined loads to guide development of lighter, tougher suspension components. Together, these studies trace a clear trajectory toward innovative, high-performance and environmentally minded suspension solutions.

Basalt fiber has gained traction as a cost-effective alternative to carbon with advantages over glass. Aref [6] and Acar [7] reviewed its processing routes and property profile. Pelin and Pelin [8] quantified the behavior of epoxy–basalt laminates under various loads, while Ţăranu [9] reported longitudinal stiffness for unidirectionally reinforced polymer composites in tension.

Analytical treatments of perforated laminates have advanced steadily. Whitney [10] proposed an empirical failure-stress model, later refined by Nuismer and Whitney [11]. Kaltakci [12] analyzed how lay-up affects stress-concentration factors around circular holes. Approximate closed-form solutions include Green and Zerna [13]. Further developments—drawing on Lekhnitskii's complex potentials Lekhnitskii [14] were offered by Yao and Yu [15], Ukadgaonker [16] and Sharma [17]. The doctoral thesis of Boubeker [18], together with the study by Harkati [19], investigates negative Poisson's ratio and non-auxetic composite materials. Relevant material data are

compiled by Gibson [20].

This work examines one reinforcement, focusing on through-thickness properties, fiber-orientation effects, Poisson-ratio influence and intermediate anisotropy. Circumferential stress fields around the hole will be mapped basalt-reinforced laminates to identify lay-ups that best mitigate stress amplification in the target geometry.

2 Analytical formulation

Although classical laminated plate theory under plane stress conditions is commonly used to describe the elastic behavior of composites, it neglects through-thickness stresses and strains. This simplification may be inadequate when out-of-plane elastic moduli are significant. To overcome this limitation, a simplified analysis is proposed that integrates the two-dimensional laminate theory with the three-dimensional constitutive laws for anisotropic materials. The aim is to evaluate the axial forces in symmetric laminates while considering variations in the Poisson's ratios associated with thickness in directions outside the principal plane.

2.1 Calculation of the out-of-plane poisson´s ratios (ν_{xz}, ν_{yz}) using thickness dimension information

Considering materials with a single plane of symmetry, the strains that manifest in the plane of each k^{th} layer are a consequence of the properties of the overall laminate and the axial force applied to it. This methodology enables the evaluation, for instance, of axial forces in symmetric laminates under different loading conditions, while accounting for the variation of Poisson's ratio in the thickness direction. For symmetric composite laminates subjected to axial loading, the mid-plane stresses, as described by laminate theory according to Herakovich [22] also applied in Harkati [19] lead to the following relationships:

$$\begin{pmatrix} \varepsilon_1 \\ \varepsilon_2 \\ \gamma_{12} \end{pmatrix} = \begin{bmatrix} A_{11} & A_{12} & A_{16} \\ A_{12} & A_{22} & A_{26} \\ A_{16} & A_{26} & A_{66} \end{bmatrix}^{-1} \begin{pmatrix} N_1 \\ N_2 \\ 0 \end{pmatrix} \tag{1}$$

The A matrix is defined as:

$$A_{ij} = \sum_{k=1}^{N} Q_{ij}^{k} t^{k} \tag{2}$$

where N is the total number of layers, Q_{ij}^{k} are the stiffness coefficients for the kth layer, and t^{k} is the individual thickness of layer k.

To determine the Poisson's ratio ν_{xz} :

$$\nu_{xz} = -\frac{\varepsilon_3}{\varepsilon_1} \tag{3}$$

where the strain ε_3 is defined as the total displacement W divided by the laminate thickness 2h. The displacement W can be expressed as Equation (4):

$$W = \int_{-h}^{h} \varepsilon_3 \, dz = \sum_{k=1}^{N} \varepsilon_3^{k} t^{k} \tag{4}$$

where $\varepsilon_3{}^{k}$ is proposed to be constant for any kth layer. In the case of plane stress, the strain $\varepsilon_z{}^{k}$ can be determined using a constitutive equation for an off-axis layer as follows:

$$\varepsilon_{zz}^{k} = S'^{k}_{31}\sigma_1^{k} + S'^{k}_{31}\sigma_1^{k} + S'^{k}_{31}\sigma_1^{k} \tag{5}$$

where S'^{k}_{ij} are the coefficients of the transformed 3D compliance matrix for the k^{th} layer.

The stresses in each layer are determined from the 2D constitutive equations and the inverse of the stiffness matrix A_{ij} is determined as:

$$\begin{pmatrix}\sigma_1\\ \sigma_2\\ \sigma_3\end{pmatrix}_k = \begin{bmatrix}Q'_{11} & Q'_{12} & Q'_{16}\\ Q'_{12} & Q'_{22} & Q'_{26}\\ Q'_{16} & Q'_{26} & Q'_{66}\end{bmatrix}^k \begin{bmatrix}A_{11} & A_{12} & A_{16}\\ A_{12} & A_{22} & A_{26}\\ A_{16} & A_{26} & A_{66}\end{bmatrix}^{-1} \begin{pmatrix}N_1\\ N_2\\ 0\end{pmatrix} \tag{6}$$

By considering N_2= 0 in Eq. (4), Eq. (5), and Eq. (6), the displacement along the three axes can be determined as:

$$W = N_1 \begin{bmatrix}(A_{21})^{-1}\\ (A_{22})^{-1}\\ (A_{26})^{-1}\end{bmatrix} \sum_{k=1}^{N}(S'_{31}S'_{32}S'_{36})^k \begin{pmatrix}Q'_{11}\\ Q'_{12}\\ Q'_{16}\end{pmatrix}^k t^k, \sum_{k=1}^{N}(S'_{31}S'_{32}S'_{36})^k \begin{pmatrix}Q'_{12}\\ Q'_{22}\\ Q'_{26}\end{pmatrix}^k t^k, \sum_{k=1}^{N}(S'_{31}S'_{32}S'_{36})^k \begin{pmatrix}Q'_{16}\\ Q'_{26}\\ Q'_{66}\end{pmatrix}^k t^k \tag{7}$$

Dividing by the axial strain ε_1 and the total laminate thickness 2h yields the through-thickness Poisson's ratio of the laminate:

$$v_{xz} = -\frac{1}{2h(A_{11})^{-1}} W \tag{8}$$

Similarly, for the Poisson's ratio v_{yz}, the total displacement W can be expressed as:

$$W = N_1 \begin{bmatrix}(A_{21})^{-1}\\ (A_{22})^{-1}\\ (A_{26})^{-1}\end{bmatrix} \sum_{k=1}^{N}(S'_{31}S'_{32}S'_{36})^k \begin{pmatrix}Q'_{11}\\ Q'_{12}\\ Q'_{16}\end{pmatrix}^k t^k, \sum_{k=1}^{N}(S'_{31}S'_{32}S'_{36})^k \begin{pmatrix}Q'_{12}\\ Q'_{22}\\ Q'_{26}\end{pmatrix}^k t^k, \sum_{k=1}^{N}(S'_{31}S'_{32}S'_{36})^k \begin{pmatrix}Q'_{16}\\ Q'_{26}\\ Q'_{66}\end{pmatrix}^k t^k \tag{9}$$

Poisson's ratio in the yz plane is defined as:

$$v_{yz} = -\frac{1}{2h(A_{22})^{-1}} W \tag{10}$$

2.2 Behavior of composite panels with round hole

To demonstrate the theoretical impact of circular holes on the mechanical behavior of perforated composite plates under uniaxial and biaxial loading as represented in Figure 1, the Lekhnitskii approximation was employed Lekhnitskii [14]. This method was used to analyze stress distribution in an orthotropic plate with a circular hole. The plate was subjected to uniaxial tensile loading with a nominal stress σ^{∞}, applied at an angle φ relative to the principal material axis.

The stress concentration factor K_f, according to Lekhnitskii [14], can be expressed by the following Eq. (11):

$$K_f = \frac{\sigma^{\alpha}}{\sigma^{\infty}} = \frac{E_{\alpha}}{E_1}[-\cos^2\varphi + (m+n)\sin^2\varphi]m\cos^2\alpha + [(1+n)\cos^2\varphi - m\sin^2\varphi]\sin^2\alpha - n(1+m+n)\sin\varphi\cos\varphi\sin\alpha\cos\alpha \tag{11}$$

where E_{α} is the modulus of elasticity in the direction defined by the angle α, which can be expressed as:

$$\frac{E_{\alpha}}{E_1} = \frac{1}{\sin^4\alpha + \frac{E_1}{E_2} + \cos^4\alpha + \frac{1}{4}(\frac{E_1}{G_{12}} - 2v_{12})\sin^2 2\alpha} \tag{12}$$

where φ is the angle at which the tensile force is applied with respect to the principal axis, and the location of the stress concentration factor is indicated by α. The coefficients m and n are given by the relationship:

$$m = \sqrt{\frac{E_x}{E_y}} \tag{13}$$

and,

$$n = \sqrt{2\left(\sqrt{\frac{E_x}{E_y}} - v_{xy}\right) + \frac{E_x}{G_{xy}}} \tag{14}$$

The effect of biaxial loading on the variation of the stress concentration factor is also investigated, as the stress concentration around the edge of circular holes in orthotropic plates is strongly influenced by the biaxiality ratio. The plate is subjected to nominal biaxial stresses p and q, with λ representing the biaxiality ratio q/p.

The stress concentration factors at the boundaries A and B of the hole, as a function of the biaxial loads p and q for isotropic and orthotropic plates, are given respectively by Lekhnitskii [14]:

$$K_A = \frac{1}{m}[-1 + \lambda(m + n)] \tag{15}$$

and,

$$K_B = 1 + n - \lambda m \tag{16}$$

The polynomial equation for the approximate distribution of normal stress along the x and y-axes of the laminate under biaxial loading is given by the relationship developed in the literature by Soutis [22] for $\lambda = 1$:

$$K_f = \frac{E_\alpha}{E_1}[m((m + n)\,cos^2\,\alpha - 1) + (1 + n)\,sen^2\,\alpha)] \tag{17}$$

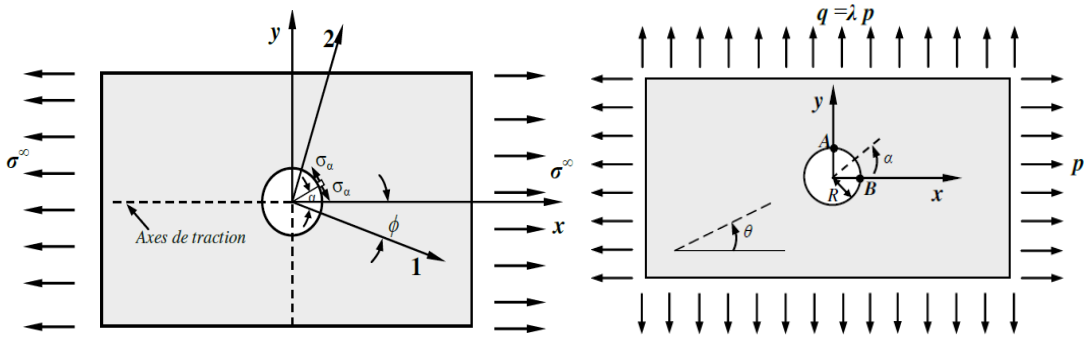


Figure 1. Geometry of the perforated plate under uniaxial loading (right) and biaxial loading (left), from Boubeker [19]

3 Materials and stacking sequence used

Table 1 shows the properties of the pre-impregnated with resin that are to be implemented and compared in the analytical model. In this case, a fiber volume fraction of 50% , 60%, 70% was considered for both materials, using the same matrix type. The elastic constants of the laminae, derived from the constituent materials using micromechanical relations, were obtained through the Mech-Gcomp™ software, as described in Angrizani [23].

Table 1. Characteristics of uniaxial prepregs used for the calculations

Elastic Modules	Fiber Type		
	Basalt/epoxy Vf = 50%	Basalt/epoxy Vf = 60%	Basalt/epoxy Vf = 70%
E_1, MPa	46.18	54.70	63.30
E_2, MPa	6.457	7.927	10.27
E_3, MPa	6.457	7.927	10.27
G_{12}, MPa	3.893	4.892	6.402
G_{13}, MPa	3.893	4.892	6.402
G_{23}, MPa	2.409	2.957	3.832
ν_{12}	0.32	0.32	0.31
ν_{13}	0.32	0.32	0.31
ν_{23}	0.34	0.34	0.34

4 Effect of material, stacking and fiber type on Poisson's ratio

The type of reinforcement and the orientation of the fibers have a significant impact on the ν_{xz}. Thus, a systematic study was conducted on symmetrical stack configurations of angular layers $(\pm\theta_2)_s$. Each laminate consisted of 37 layers, with fiber orientation angles increased by 5°. A type of reinforcing material was evaluated considering its potential applications: basalt, with fiber volume fractions of 50%, 60%, and 70%, alongside an epoxy resin matrix.

The basalt/epoxy composite exhibits classical behavior. However, the objective of this study is to identify a fiber orientation configuration that minimizes deformation in the region around the central hole. It is noted, as shown in Figure 2, that the region where the Poisson's coefficient ν_{xz} is the lowest possible is at 30°, varying from 0.108 for a 50% basalt fiber volume fraction, 0.120 for 60% basalt, and 0.140 for 70% basalt.

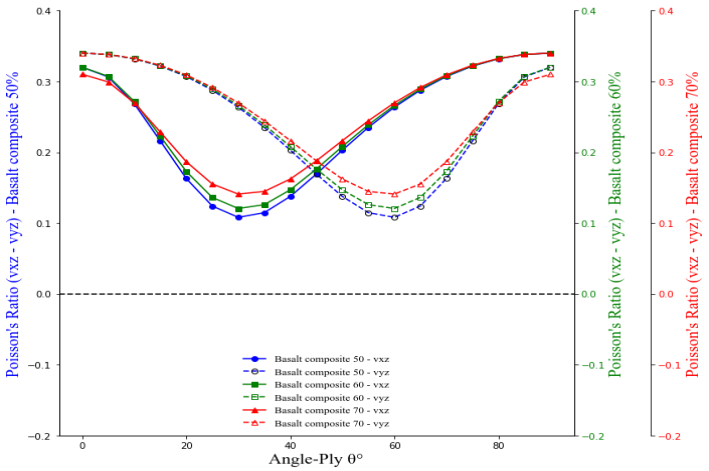


Figure 2. Influence of fiber orientation and reinforcement type on ν_{xz} for laminates $(\pm\theta_2)_s$

5 Effect of the Orientation of any Type of Material on the Stress Concentration Factor

Figure 3 presents the results of the influence of fiber orientation and level of anisotropy in the plane, for both types of loading (uniaxial and biaxial). The orientation of the fiber within the layer determines where the maximum value of the stress concentration factor (K_f) is located. For the material investigated, the maximum value of the stress concentration factor is achieved with a fiber orientation of $\theta = 0°$ under uniaxial loading and $\theta = 45°$ under biaxial loading; K_f reaches a peak corresponding to a fiber orientation of $\theta = 45°$. The fiber used and its orientation

play a crucial role in achieving the lowest possible Poisson's ratio.

For different reasons of anisotropy in unidirectional laminates ($\pm\theta_2$), Figure 3 shows the fluctuation of K_f as a function of the fiber orientation angle—on the left for unidirectional laminates and on the right for bidirectional laminates. The increase in layer anisotropy has a significant effect on K_f. K_f is significantly influenced by the medium's anisotropy, rapidly decreasing with the increase in layer orientation.

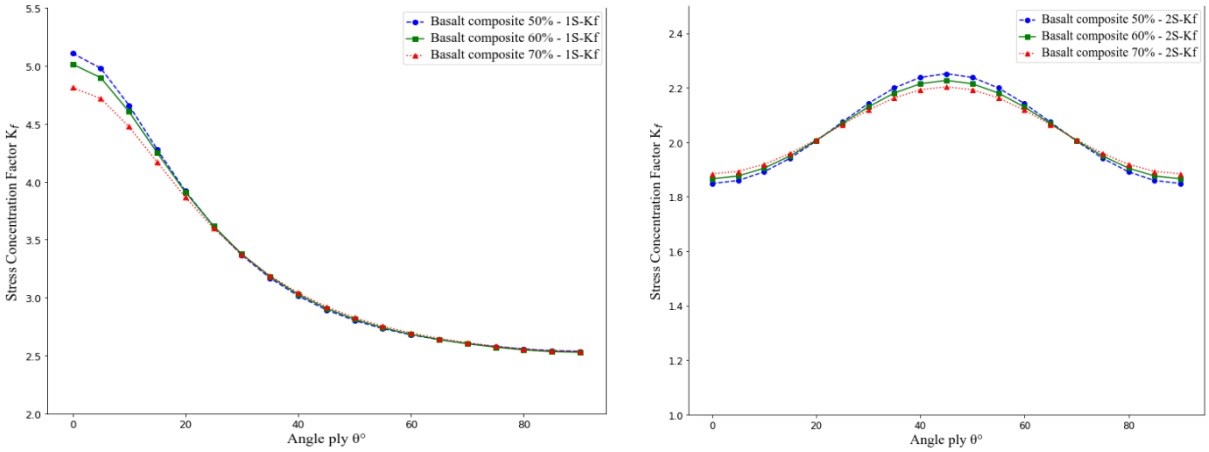


Figure 3. K_f versus θ for Basalt composite, under uniaxial loading (right) and biaxial loading (left)

6 Effect of the type of reinforcement on Poisson's ratio v_{xz}

Figure 5 illustrates the relationship between the stress concentration factor and the out-of-plane Poisson's ratio for each stacking sequence. The K_f for a Basalt composite 70% laminate under uniaxial loading decreases by 30% when the Poisson's ratio v_{xz} varies from 0.14 to 0.31 at 0° and 30°, while for Basalt composite 60% it decreases by 33% when v_{xz} varies from 0.12 to 0.32 at 0° and 30° and Basalt composite 50% it decreases by 34% when v_{xz} varies from 0.10 to 0.32 at 0° and 30°. The (±30) for Basalt fiber exhibited the highest energy release rate. However, when the through-thickness Poisson's ratio v_{xz} is positive, contraction occurs both in thickness and width directions, increasing the stress concentration level at the crack tip.

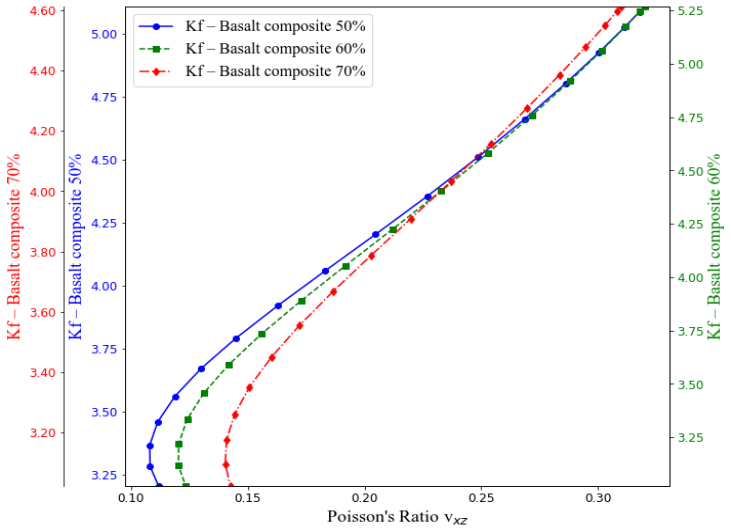


Figure 5. Variation of K_f as a function of v_{xz} in a plate subjected to uniaxial tensile loading

7 Conclusions

This investigation into the mechanical behavior of basalt composite laminates highlights the critical influence of material properties and laminate architecture on stress distribution. The observed trends highlight how specific variations in the material elastic response significantly impact localized stress at critical points in the structure and how fiber volume affects properties. The investigation presented here is a work in progress. The analysis is intended to give technical support on the viability of producing composite leaf springs made of basalt fibers and how different fiber orientations influence stress concentration factors in circular holes that are presented in the spring design. Mitigating the stress factors are a crucial key to develop efficient products.

Acknowledgements. The authors acknowledge the support of Conselho Nacional de Desenvolvimento Científico e Tecnológico (CNPq), Coordenação de Aperfeiçoamento de Pessoal de Nível Superior (CAPES), Instituto Hercílio Randon (IHR) and Universidade Federal do Rio Grande do Sul (UFRGS) for the financial support provided throughout the development of this work.

Authorship statement. The authors hereby confirm that they are the sole liable people responsible for the authorship of this work, and that all material that has been herein included as part of the present paper is either the property (and authorship) of the authors or has the permission of the owners to be included here.

References

[1] K. K. Chawla. Composite Materials: Science and Engineering, 4th ed. Springer Nature Switzerland AG, 2019.
[2] Society of Automotive Engineers – Spring Committee. Spring Design Manual, 2nd ed. SAE International, 1996.
[3] J. Ke, Z.-Y. Wu, X.-Y. Chen and Z.-P. Ying, "A review on material selection, design method and performance investigation of composite leaf springs". Composite Structures, vol. 226, art. 111277, 2019.
[4] B. Tadesse and O. Fatoba, "Design optimization and numerical analyses of composite leaf spring in a heavy-duty truck vehicle". Materials Today: Proceedings, vol. 62, n. 6, pp. 2814–2821, 2022.
[5] E. D. Telli, G. P. Mezzomo, D. M. de Leon, J. M. Vassoler, E. M. Rech, J. Boaretto, A. Sakata and I. Iturrioz, "Strength assessment of composite beams under combined loads for application in mechanical suspension systems". Engineering Failure Analysis, vol. 177, 2025.
[6] C. Aref, "Glass Fibers". In: Fiber Technology for Fiber-Reinforced Composites, 1st ed., pp. 99–121. Elsevier, 2017.
[7] V. Acar, F. Cakir, E. Alyamaç and M. Ö. Seydibeyoğlu, "Basalt Fibers". In: Fiber Technology for Fiber-Reinforced Composites, 1st ed., pp. 169–185. Elsevier, 2017.
[8] C.-E. Pelin and G. Pelin, "Mechanical properties of basalt fiber/epoxy resin composites". INCAS Bulletin, vol. 16, n. 2, pp. 101–110, 2024.
[9] N. Ţăranu, R. Hohan and L. Bejan, "Longitudinal stiffness characteristics of unidirectional fibre reinforced polymeric composites subjected to tension". Buletinul Institutului Politehnic Din Iaşi, vol. LVIII(LXII)(2), 41-46, 2012.
[10] R. J. Nuismer and J. M. Whitney, "Uniaxial Failure of Composite Laminates Containing Stress Concentrations". In: Fracture Mechanics of Composites, pp. 117–142. ASTM, 1975.
[11] J. M. Whitney and R. J. Nuismer, "Stress Fracture Criteria for Laminated Composites Containing Stress Concentrations". Journal of Composite Materials, vol. 8, n. 3, pp. 253–265, 1974.
[12] M. Y. Kaltakci, "Stress analysis of orthotropic laminates with a circular hole under biaxial loading". Computers & Structures, vol. 61, n. 1, pp. 67–74, 1996.
[13] A. E. Green and W. Zerna. Theoretical Elasticity. Clarendon Press, 1954.
[14] S. G. Lekhnitskii, S. W. Tsai and T. Cheron. Anisotropic Plates. Routledge, Gordon and Breach Science, 1984.
[15] Y. Weixing and Y. Xinlu, "The effect of stacking sequence on the tensile failure of composite laminates with a central hole". Composites Science and Technology, vol. 41, n. 1, pp. 47–61, 1991.
[16] V. G. Ukadgaonker and D. K. N. Rao, "Stress concentrations around circular holes in composite laminates under uniaxial tension". Composite Structures, vol. 49, n. 3, pp. 339–345, 2000.
[17] D. S. Sharma, "Stress concentration around circular/elliptical/triangular cutouts in infinite composite plate". In: Proceedings of the World Congress on Engineering, WCE. London, UK, 2011.
[18] R. Boubeker. Etude Expérimentale et Numérique du Comportement des Plaques Trouées en Matériaux Composites (in French). Doctoral thesis, Université Mohamed Khider, Biskra, 2016.
[19] A. Harkati, S. Chouai, E.-H. Harkati, A. Bezazi, S. Ellagoune and F. Scarpa, "Using a Negative Poisson's Ratio to Mitigate Stress Concentrations in Perforated Composite Plates". Physica Status Solidi B: Basic Solid State Physics, vol. 261, n. 7, art. 2400115, 2024.
[20] A. G. Gibson, "Through-thickness elastic constants of composite laminates". Journal of Composite Materials, vol. 47, n. 28, pp. 3487–3499, 2012.
[21] C. T. Herakovich. Mechanics of Fibrous Composites. Wiley, 1998.

[22] C. Soutis and C. Filiou, “Stress distributions around holes in composite laminates subjected to biaxial loading”. Applied Composite Materials, vol. 5, p. 365, 1998.
[23] C. C. Angrizani, E. A. W. de Menezes, F. F. Luz, A. A. Muller and S. C. Amico, “Use of the academic software Mech-GComp for teaching particulate composites (in Portuguese)”. Revista de Ensino de Engenharia, vol. 36, n. 1, 2017.